Hydroperoxides. Although the hydroperoxides have been isolated as a mixture of isomers, complete characterization was not possible because of decomposition. Strong evidence in support of their structure comes from NMR analysis: ^{1}H NMR, 8.15, 8.10, and 7.92 ppm (br s) consistent with hydroperoxidic protons; 6.76, 6.30, 5.82, 5.50, and 5.32 ppm (presumably vinylic protons with very complex splitting patterns); 4.80 and 4.54 ppm (allylic protons α to oxygen); 1.73 and 1.26 ppm (alkyl protons, multiplicities could not be established because of overlapping peaks). ^{13}C NMR, peaks are also consistent with the assigned structure; 138-126 ppm (substituted olefinic carbons), 119.7 and 119.4 ppm (terminal alkene carbons); 87-80 ppm (oxygen-substituted allylic carbons); 30-18 ppm (alkyl carbons). Appropriate vinyl-vinyl, vinyl-allyl, and vinyl-alkyl couplings appear in the 2-D COSY (^{1}H-^{1}H) NMR at -20 °C.

Acknowledgment. Supported in part by NSF Grant No. CHE86-11873.

Registry No. A, 88078-74-4; B, 88078-75-5; *cis*-C, 15798-64-8; *trans*-C, 123-73-9; D, 75-07-0; E, 116053-72-6; (*E*,*E*)-2,4-hexadiene, 5194-51-4; (*E*,*Z*)-2,4-hexadiene, 5194-50-3; (*Z*,*Z*)-2,4-hexadiene, 6108-61-8.

Photolabile 1-(2-Nitrophenyl)ethyl Phosphate Esters of Adenine Nucleotide Analogues. Synthesis and Mechanism of Photolysis

Jeffery W. Walker, Gordon P. Reid, James A. McCray,† and David R. Trentham*

Contribution from the National Institute for Medical Research, Mill Hill, London NW7 1AA, United Kingdom. *Received March 30, 1987*

Abstract: A general method is described for preparing photolabile 1-(2-nitrophenyl)ethyl esters of phosphate and thiophosphate compounds. The method is based on selective alkylation of weakly ionizing phosphate groups by a new alkylating agent, 1-(2-nitrophenyl)diazoethane. ATP and the widely used structural analogues of ATP, 5'-adenylyl imidodiphosphate (ATP(β,γNH)) and adenosine 5'-(3-thiotriphosphate) (ATP(γS)), were alkylated on the terminal (γ) phosphate group. ATP(γS) was alkylated on oxygen or on sulfur in approximately equal amounts. Photolysis of P^3-1-(2-nitrophenyl)ethyladenosine 5'-triphosphate, commonly called "caged ATP", was analyzed spectroscopically at pH values close to neutral in aqueous solvents by use of laser pulse photolysis. The kinetics of formation of the three products, ATP, 2-nitrosoacetophenone, and H^+, were each monitored, as well as the kinetics of formation and decay of an intermediate presumed to be an *aci*-nitro compound (apparent ϵ_{406nm} = 9.1×10^3 M^{-1} cm^{-1}). For caged ATP in the presence of 3 mM $MgCl_2$, the *aci*-nitro intermediate and H^+ formed first at $>10^5$ s^{-1} followed by the decay of the intermediate at 86 s^{-1} at pH 7.1, 21 °C, and ionic strength 0.18 M. ATP, monitored by a biochemical assay, and 2-nitrosoacetophenone, monitored by a characteristic absorption band at 740 nm, were formed simultaneously with the decay of the intermediate under all conditions tested. The rate of decay of the *aci*-nitro intermediate was therefore used as a measure of the rate of release of the nucleotide analogues from their photolabile precursors. At pH 7.1, 0.18 M ionic strength, and 21 °C the rate constants ranged from 35 to 250 s^{-1} and displayed a similar dependence on pH as caged ATP. The steady-state quantum yields of the 1-(2-nitrophenyl)ethyl phosphate esters were in the range 0.49-0.63. The deleterious effect of 2-nitrosoacetophenone on biological materials can be avoided by having thiols present. The reaction kinetics of dithiothreitol and 2-nitrosoacetophenone was described by a two-step process, the first step having a rate constant of 3.5×10^3 M^{-1} s^{-1} and the second 45 s^{-1} at pH 7.0, 21 °C, and ionic strength 0.18 M.

An emerging technique in biochemical research is the controlled release of substrates within intact biological systems by rapid photolysis of photolabile precursors (reviewed by Gurney and Lester[1]). One of the first photolabile precursors of an important biological substrate, ATP, was the 1-(2-nitrophenyl)ethyl P^3-ester of ATP, I, commonly termed "caged ATP", that on photolysis releases ATP at 220 s^{-1} at pH 7 and 21 °C.[2] This property of caged ATP together with the high-energy output and time resolution afforded by lasers have permitted a range of physiological experiments where diffusional delays of ATP may be overcome by the use of caged ATP. For example, the mechanism of force transduction in muscle has been studied extensively by this approach[3] where up to 77% conversion of caged ATP to form several millimolar ATP can be achieved in a single laser pulse.[4]

2-Nitrobenzyl photochemistry has provided the basis for kinetic studies of other physiological systems. Variations on the caged ATP theme include its application to cyclic nucleotides,[5] protons,[6] Ca^{2+},[7] carbachol,[8] *myo*-inositol 1,4,5-triphosphate,[9] and photosensitive Ca^{2+} channel blockers.[10] However, a major limitation to a more general application of this approach to a variety of regulatory cellular processes has been the considerable time required for synthesis and characterization of new compounds. We

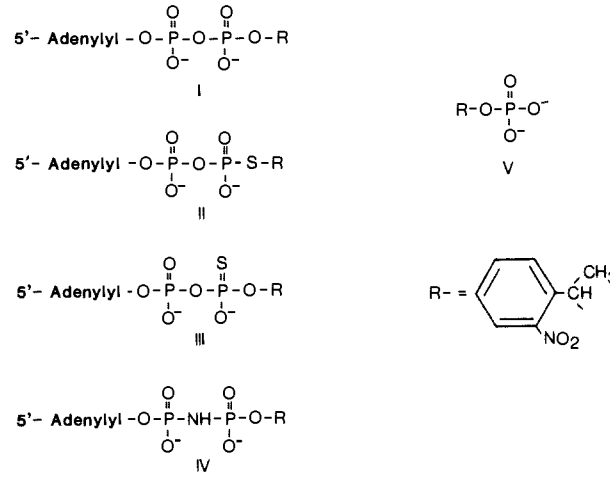

† Present address: Department of Physics, Drexel University, Philadelphia, PA 19104.

(1) Gurney, A. M.; Lester, H. A. *Physiol. Rev.* **1987**, *67*, 583-617.

0002-7863/88/1510-7170$01.50/0

now report a general method for preparing 1-(2-nitrophenyl)ethyl phosphate esters that is fast, simple, and efficient. We describe the synthesis and characterization of compounds of biological interest related to ATP: the *S*- and *O*-1-(2-nitrophenyl)ethyl P^3-esters of ATP(γS), II and III, and the 1-(2-nitrophenyl)ethyl P^3-ester of ATP(β,γNH), IV. ATP(γS)[11] and ATP(β,γNH)[12] are analogues of ATP that have found wide use in biological research as probes of biochemical mechanisms involving ATP. The photosensitive precursors of compounds prepared by this method are being used in physiological experiments to investigate mechanisms of muscle contraction and its regulation and ion conductance in sensory neurons.[13]

It is important to know the basic photochemical properties relating to quantum yield and photolysis kinetics of the new compounds, especially in relation to their potential use for physiological studies. On laser pulse photolysis of caged ATP, the yield of ATP is related to the amplitude of an absorption signal in the near-UV that occurs within 10 μs of the laser pulse and is thought to be due to an *aci*-nitro intermediate. The rate of formation of ATP appears to occur concomitant with the decay of this absorption band.[2b]

Before the amplitude of this rapid initial absorption increase and the rate of its decay can be used as an assay for the extent and rate of formation of ATP analogues on photolysis of their photolabile precursors, the extinction coefficient of the intermediate and the validity of the kinetic assay must be established. One reason for questioning its validity is that the decay of the *aci*-nitro intermediate, IX, is most unlikely to be a single-step nucleophilic vinylic substitution at an sp^2-carbon atom that is implicit in a direct displacement of the $-YPO_3^-$ group from IX.[14] A series of kinetic assays of ATP, nitroso group, and H^+ formation are used to formulate a minimal mechanism for caged ATP photolysis that also accommodates the pH dependence of the photolysis kinetics.

A complication in the use of 1-(2-nitrophenyl)ethyl esters for physiological studies is that the photolysis byproduct, 2-nitrosoacetophenone (XI), reacts with biological compounds.[2a] This can be avoided by use of thiols that react rapidly but in a complex manner with nitroso ketones. This reaction is also analyzed.

Materials and Methods

Nucleotides were obtained from Sigma Chemical Co., except ATP(γS) and ATP(β,γNH) (obtained from Boehringer-Mannheim), and used without further purification.

HPLC was carried out with a Waters 6000A solvent delivery system, sample injector, and UV absorbance detector at 254 nm. For reversed-phase chromatography, Merck RP8 or Waters C_{18} μ Bondapak columns were used; ion-exchange separations on Whatman partisil 10 SAX columns were employed with isocratic elution.

Proton NMR spectra were obtained on Bruker 270- or 500-MHz instruments, and chemical shifts are relative to internal reference compounds, tetramethylsilane in $CDCl_3$ or dimethyl-d_6 sulfoxide, and 3-(trimethylsilyl)propanesulfonate (sodium salt) in D_2O. ^{31}P NMR spectra were recorded as described in Table II.

Photolysis was effected by frequency doubling the output of either a ruby laser[2b] or a Candela (Model 1050) dye laser that was frequency doubled to provide a 1-μs pulse of 25–60 mJ at 320 nm. This was accomplished by doubling the dye laser cavity length by folding the beam back 180° with the use of three dispersive SF-10 (n = 1.72) equilateral prisms. Rhodamine 640 dye (20 μM) obtained from Exciton Corp. was dissolved in ethanol–water (1:1, v/v). The polarized, frequency-narrowed primary laser output was of the order of 500 mJ at 640 nm. This laser output beam was then line-focused by a fused silica cylindrical lens onto a 5 cm long by 2 cm^2 ADP (ammonium dihydrogen phosphate) frequency-doubling crystal that was cut at a nominal value of 54° for angle tuning and first index matching conditions. The crystal was obtained from Quantum Technology Inc. and was hermetically sealed in a dry nitrogen atmosphere in a temperature-controlled oven. The laser light emanating from the ADP crystal was then recollimated with a fused silica cylindrical lens and the fundamental 640-nm laser light separated from the desired secondary 320-nm laser light with the use of either a Schott 5181 glass filter or compensating quartz plate Brewster stacks. Output of the secondary beam was measured with an Rj-7100 energy meter (Laser Precision Corp.).

An absorption spectrophotometer was linked to the dye laser. The incident light from a tungsten iodide lamp was first passed through a 5031 Corning blue glass filter (peak transmission of 42% at 406 nm and <0.2% below 345 nm) for near-UV observations or a 400 nm Schott cut-off filter for longer wavelength observations. Light was then transmitted through a 4-mm× observation cell orthogonal to the laser beam and into a monochromator and detected by an EMI 9601B photomultiplier except when the nitroso absorption band at 740 nm was being monitored when a Hamamatsu R316 photomultiplier was used.

A fluorescence spectrometer was linked to the ruby laser. For this spectrometer the same 4-mm quartz cell with polished sides and base was used. The laser pulse irradiated the cell in the horizontal plane. The exciting light from a PRA 150-W xenon arc lamp was passed through a water heat filter, an optical shutter (to protect the interference filter), a 366-nm interference filter, and a liquid light guide and irradiated the cell in a vertical orientation through the base of the cell. The fluorescence was then monitored in the horizontal plane orthogonal to both the exciting and laser light. The emitted light was passed through a 406-nm interference filter and detected by an EMI 9601B photomultiplier.

In each spectrophotometer, after I–V conversion, signals were recorded with digital and/or analog storage oscilloscopes. Data were analyzed by use of a nonlinear least-squares fit to the exponential traces.[16] Transients were computer averaged in the case of nitroso ketone reactions recorded at 740 nm.

Steady-state photolysis was carried out in a 1-cm quartz cuvette housed 25 cm from a 150-W xenon arc lamp. Light from the lamp was passed through a water heat filter and a Corning 9863 glass band-pass filter (300–350 nm) and focused onto the cuvette. Absorption spectra were recorded on a Beckman DU8 spectrophotometer. The fluorescence stopped-flow equipment was as described by Whitaker et al.[17] Elemental analysis was done by Butterworth Laboratories Ltd.

Hydrazone of 2-Nitroacetophenone (VI). To 8.26 g of 2-nitroacetophenone (Aldrich; 0.05 mol) in 100 mL of 95% ethanol was added 5.62 g of hydrazine hydrate (0.112 mol) and 3.2 mL of glacial acetic acid (0.05 mol), and the mixture was heated under reflux for 3 h. Ethanol was evaporated off under vacuum, and the residue was partitioned between $CHCl_3/H_2O$ to remove hydrazine acetate. The $CHCl_3$ phase was evaporated to dryness and the product distilled [118 °C (0.22 mmHg)] and stored at −20 °C: yield 95%; UV (ethanol) $\epsilon = 9.4 \times 10^3$ M^{-1} cm^{-1} at λ_{max} = 248 nm. NMR spectrum in dimethyl-d_6 sulfoxide revealed a mixture of two similar compounds in a ratio of 3.2:1 (25 °C) that was unchanged after fractional distillation. The ratio was altered to 1.9:1 by increasing the temperature to 90 °C during the NMR measurements. This temperature effect was reversible, suggesting that interconversion of two forms of the hydrazone was occurring; these forms probably

(2) (a) Kaplan, J. H.; Forbush, B., III; Hoffman, J. F. *Biochemistry* **1978**, *17*, 1929–1935. (b) McCray, J. A.; Herbette, L.; Kihara, T.; Trentham, D. R. *Proc. Natl. Acad. Sci. U.S.A.* **1980**, *77*, 7237–7241.
(3) (a) Goldman, Y. E.; Hibberd, M. G.; McCray, J. A.; Trentham, D. R. *Nature (London)* **1982**, *300*, 701–705. (b) Hibberd, M. G.; Trentham, D. R. *Annu. Rev. Biophys. Biophys. Chem.* **1986**, *15*, 119–161.
(4) Ferenczi, M. A.; Homsher, E.; Trentham, D. R. *J. Physiol.* **1984**, *352*, 575–599.
(5) (a) Engels, J.; Schlaeger, E.-J. *J. Med. Chem.* **1977**, *20*, 907–911. (b) Nerbonne, J. M.; Richard, S.; Nargeot, J.; Lester, H. A. *Nature (London)* **1984**, *310*, 74–76.
(6) (a) McCray, J. A.; Trentham, D. R. *Biophys. J.* **1985**, *47*, 406a. (b) Khan, S.; Meister, M.; Berg, H. C. *J. Mol. Biol.* **1985**, *184*, 645–656. (c) Shimada, K.; Berg, H. C. *J. Mol. Biol.* **1987**, *193*, 585–589.
(7) (a) Tsien, R. Y.; Zucker, R. S. *Biophys. J.* **1986**, *50*, 843–853. (b) Gurney, A. M.; Tsien, R. Y.; Lester, H. A. *Proc. Natl. Acad. Sci. U.S.A.* **1987**, *84*, 3496–3500.
(8) Walker, J. W.; McCray, J. A.; Hess, G. P. *Biochemistry* **1986**, *25*, 1799–1805.
(9) Walker, J. W.; Somlyo, A. V.; Goldman, Y. E.; Somlyo, A. P.; Trentham, D. R. *Nature (London)* **1987**, *327*, 249–252.
(10) (a) Morad, M.; Goldman, Y. E.; Trentham, D. R. *Nature (London)* **1983**, *304*, 635–638. (b) Gurney, A. M.; Nerbonne, J. M.; Lester, H. A. *J. Gen. Physiol.* **1985**, *86*, 353–379.
(11) (a) Eckstein, F. *Acc. Chem. Res.* **1979**, *12*, 204–210. (b) Eckstein, F. *Trends Biochem. Sci.* **1980**, *5*, 157–159. (c) Goody, R. S.; Eckstein, F. *J. Am. Chem. Soc.* **1971**, *93*, 6252–6257.
(12) (a) Yount, R. G.; Babcock, D.; Ballantyne, W.; Ojala, D. *Biochemistry* **1971**, *10*, 2484–2489. (b) Yount, R. G. *Adv. Enzymol.* **1975**, *43*, 1–56.
(13) (a) Dantzig, J. A.; Walker, J. W.; Trentham, D. R.; Goldman, Y. E. *Proc. Natl. Acad. Sci. U.S.A.* **1988**, *85*, 6716–6720. (b) Dolphin, A. C.; Wootton, J. F.; Scott, R. H.; Trentham, D. R. *Pflügers Archiv.* **1988**, *411*, 628–636.
(14) (a) Rappaport, Z. *Acc. Chem. Res.* **1981**, *14*, 7–15. (b) Cohen, D.; Bar, R.; Shaik, S. S. *J. Am. Chem. Soc.* **1986**, *108*, 231–240.
(15) Klein, R. M. *Photochem. Photobiol.* **1975**, *29*, 1053–1054.
(16) Hardman, M. J.; Coates, J. H.; Gutfreund, H. *Biochem. J.* **1978**, *171*, 215–223.
(17) Whitaker, J. R.; Yates, D. W.; Bennett, N. G.; Holbrook, J. J.; Gutfreund, H. *Biochem. J.* **1974**, *139*, 677–697.

represent *E* (anti) and *Z* (syn) isomers about the C=N bond. ^{1}H NMR δ 7.30–7.55 (4 H, aromatic), 6.64 and 5.54 (3.2:1; br s, 2 H (exchangeable in D_2O in spectrum measured in $CDCl_3$, amine), 2.03 and 2.17 (3.2:1; s, 3 H, methyl). Anal. ($C_8H_9N_3O_2$) C, H, N.

1-(2-Nitrophenyl)diazoethane (VII). Hydrazone VI was oxidized with MnO_2 by the method of Jugelt and Berseck.[18a] Reproducible oxidations in high yield (>95% by ^{1}H NMR analysis of a reaction run in $CDCl_3$) were obtained with an activated grade of MnO_2 from BDH Merck (product No. 805958; used without further purification). Hydrazone (0.715 g, 4.0 mmol) in 50 mL of $CHCl_3$ was stirred with 2.85 g of MnO_2 (33 mmol) for 5 min in the dark. (All manipulations from this point on were carried out in a dark room; products were stored in brown glass vials wrapped in foil.) MnO_2 was removed by filtration, and the $CHCl_3$ filtrate was washed with 0.1 M $NaHCO_3$ pH 7, dried over $MgSO_4$, and stored at −20 °C. At 21 °C the decomposition rate of VII was 3.5×10^{-6} s^{-1}, $t_{1/2}$ = 2.3 days.[18b] Spectra: UV (ethanol) $\epsilon = 1.3 \times 10^3$ M^{-1} cm^{-1} at λ_{max} = 405 nm, $\epsilon = 8.7 \times 10^3$ M^{-1} cm^{-1} at λ_{max} = 272 nm; IR (C=N^+=N^-) 2050 cm^{-1}; NMR ($CDCl_3$) δ 6.95–7.60 (4 H, aromatic), 2.10 (s, 3 H, methyl).

1-(2-Nitrophenyl)ethyl Phosphate Diesters. Standard Method for Caged Nucleotides. Nucleotides were converted to their acid form by treatment with Dowex 50 W (hydrogen form). Of this aqueous solution, 3 mL containing 0.1–1 mmol of nucleotide was adjusted to pH 4–5 with NaOH. For smaller scale reactions using expensive nucleotides (ATP(γS), ATP(β,γNH)) Dowex 50 W treatment was eliminated to minimize losses and pH adjustments were made with dilute HCl. Nucleotides were stirred vigorously with an equal volume of $CHCl_3$ containing 0.5–1.5 mmol of VII at room temperature. Progress of the reaction (aqueous phase) was monitored by analytical HPLC, giving maximum yields in 20–24 h. Yields could be increased to 100% by readjusting to pH 4 with dilute HCl and adding a fresh $CHCl_3$ solution of VII. For preparative-scale purification, the aqueous phase was removed and washed twice with $CHCl_3$ and products were isolated by chromatography on a preparative C_{18} reversed-phase HPLC column (2 cm × 30 cm) with 10 mM phosphate (pH 5.5)–methanol (85:15, v/v; with a higher proportion of methanol for singly or doubly charged caged nucleotides) and then on a DEAE-cellulose column (1.6 cm × 30 cm) eluted with a 1-L gradient of 10–700 mM triethylammonium bicarbonate (TEAB) at pH 7.5. TEAB was removed from products by rotary evaporation under vacuum with four methanol washes. The caged nucleotides were stored as frozen aqueous solutions at −20 °C.

Caged ATP(γS), II, and III. To 75 mg of ATP(γS) (tetralithium salt; 0.14 mmol containing ~20% ADP) in 2.0 mL of water at pH 4.5 was added 3 mL of $CHCl_3$ containing 0.7 mmol of VII and the resultant mixture stirred vigorously for 20 h. HPLC analysis revealed three peaks: unreacted nucleotide (15%), caged ATP(γS) (60%), and caged ADP (25%). Caged ADP arose principally from contamination of commercial ATP(γS) by ADP.[18c] Caged ATP(γS) eluted as a single peak from the preparative C_{18} column but separated into two well-resolved components on the DEAE-cellulose column. These components were characterized by their NMR spectra (Table II). S-Caged ATP(γS) eluted first as a single major peak at 200 mM TEAB, and O-caged ATP(γS) eluted at 300 mM TEAB as a second peak that was itself partially resolved into a double peak. O-Caged ATP(γS) exists as four diastereoisomers, and the double peak probably respresents at least a partial separation of these diastereoisomers. This conclusion was supported by HPLC analysis (on a SAX column eluted isocratically with 0.4 M $(NH_4)_2HPO_4$ adjusted to pH 4.0 with HCl) of samples of O-caged ATP(γS) from across the double peak. Nucleotide from the leading partially resolved peak eluted predominantly after 15 min (flow rate 1.5 mL/min) and from the trailing peak after 12.5 min. Under these conditions, both of the diastereoisomers of S-caged ATP(γS) had a retention time of 12 min and that of ATP(γS) was 26 min.

Caged ATP(β,γNH) (IV). ATP(β,γNH) (tetralithium salt; 22 mg, 0.042 mmol) in 1 mL of water at pH 4.0 was stirred with 0.7 mmol of VII in 3 mL of $CHCl_3$ for 24 h. Conversion of ATP(β,γNH) to caged ATP(β,γNH) was 85% by HPLC analysis of the aqueous phase. Yield of purified caged ATP(β,γNH) isolated by the two-column procedure outlined above was 34% (see Table II for NMR characterization).

1-(2-Nitrophenyl)ethyl phosphate (V) was synthesized as described previously.[4] It was further purified by DEAE-cellulose chromatography.

2-Nitrosoacetophenone (XI) was prepared by photolysis at 300–350 nm of aqueous solutions of either I or V with frequent extraction into $CHCl_3$ (or $CDCl_3$) that was protected from light. The photolysis was followed either by monitoring the methyl group of XI by ^{1}H NMR in $CDCl_3$ or by HPLC analysis of the aqueous phase.

Table I. Photochemical Properties of Caged Compounds[a]

	Q_p[b]	rel A_{406nm}[c]	k(pH 7.1),[d] s^{-1}
caged ATP, I[e]	0.63	1	86
S-caged ATP(γS), II	0.57	0.9	35
O-caged ATP(γS), III	0.49	0.8	105
caged ATP(β,γNH), IV	0.52	0.9	250
caged AMP[f]	0.51	0.85	200
caged P_i, V	0.54	0.85	80000[g]

[a] Q_p, rel A_{406nm}, and k were measured under standard conditions at 21 °C: 140 mM KCl, 3 mM $MgCl_2$, 100 mM TES adjusted to pH 7.1 with KOH. [b] Q_p represents the product quantum yield measured relative to caged P_i by steady-state irradiation of each compound mixed with caged P_i, followed by HPLC analysis to determine the extent of conversion. Q_p = 0.54 for caged P_i.[2a] [c] rel A_{406nm} is the amplitude of the absorbance change at 406 nm normalized to that of caged ATP. rel A_{406nm} values were independent of Mg^{2+} and pH near neutrality. Errors are estimated to be ±5% for caged AMP and V and ±10% for II–IV. [d] k is a first-order rate constant obtained by least-squares analysis of the decay of absorbance at 406 nm. k values for each compound decreased 10-fold at pH 8.1. k values for I–IV (but not for caged AMP and V) increased in the absence of Mg^{2+} (see Figure 4). [e] The two diastereomers of caged ATP (resolved by C_{18} reversed-phase HPLC) had identical photolytic properties. [f] Caged AMP is the 1-(2-nitrophenyl)ethyl *P*-ester of 5′-AMP. [g] k for caged P_i was measured in the range pH 8–9.5 and was first order in H^+. The value of 80 000 s^{-1} is extrapolated from data in the pH 8–9.5 range.

Results and Discussion

Synthesis with 1-(2-Nitrophenyl)diazoethane. The new synthetic method in which the reaction is performed in mixed solvents[19] is based on selective alkylation of weakly ionizing phosphate groups by 1-(2-nitrophenyl)diazoethane (VII). VII is synthesized by a simple two-step procedure: Progress of the formation of VII

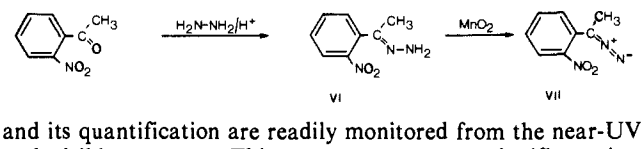

VI VII

and its quantification are readily monitored from the near-UV and visible spectra. This route represents a significant improvement over an alternate method in which (tolyl-*p*-

(18) (a) Jugelt, W.; Berseck, L. *Tetrahedron* **1970**, *26*, 5581–5586. (b) Additional points relating to 1-(2-nitrophenyl)diazoethane synthesis and use are as follows. Other grades of MnO_2 activated for oxidation (e.g., Aldrich 21,746-6) could be used, but yields of diazoethane were variable even after base treatment and washing to neutrality. For use of the diazoethane in syntheses it was not necessary to wash with bicarbonate. MnO_2 caused decomposition of the diazoethane at 5×10^{-5} s^{-1} at 21 °C. The absorption band at 405 nm provided the most convenient means of following the concentration of diazoethane since no other components of the reaction mixture absorbed at 405 nm. Protection from daylight was essential for the diazoethane. In the case of the caged compounds, exposure to subdued daylight for a few minutes did not induce significant photolysis. The synthesis may also be done in diethyl ether (see ref 18c). In general, caution is needed in handling diazoethanes. We have experienced no explosions in 2 years of frequent use. However, we have not operated on more than a 4-mmol scale and have only rarely evaporated off an organic solvent, and then with caution. (c) Conditions chosen were those in which the alkylation of ATP(γS) was favored compared to ATP(γS) hydrolysis to ADP. The rates of ATP(γS) hydrolysis in water at 21 °C were approximately 0.29, 0.22, 0.20, 0.094, and 0.054 h^{-1} at pH 3.5, 4, 4.5, 5, and 6, respectively. Highest yields of caged ATP(γS) were obtained by alkylation of ATP(γS) at pH 4.5–5. The caged derivatives of ATP(γS) were stable with respect to hydrolysis relative to ATP(γS). The best way we have found to obtain ATP(γS) in the absence of ADP is by photolysis of caged ATP(γS) at neutral pH and extraction of byproduct 2-nitrosoacetophenone into $CHCl_3$. On the suggestion of R. S. Goody we have used a diethyl ether rather than $CHCl_3$ solution of the diazoethane. The alkylation then proceeds quantitatively with no measurable hydrolysis within 20 min. (d) Alkylations of ATP with 1-(2-nitrophenyl)-diazoethane were performed under a variety of solvent conditions. Reactions in homogeneous phase in dimethyl sulfoxide were complete within 2 hours, but some modification at sites other than the weakly acidic phosphate group occurred. In addition, the prior preparation of tris(triethylammonium) salt of ATP was an extra step in the synthesis, making this approach unsatisfactory overall. Substitution of triethylammonium and tri-*n*-butylammonium salts of ATP for Na_3ATP in the $CHCl_3/H_2O$ reaction mixture afforded no consistent kinetic advantage (i.e., parameters such as the rate of mixing had a more pronounced effect). A major kinetic advantage was achieved by using diethyl ether instead of $CHCl_3$.[18c]

(19) (a) Haines, J. A.; Reese, C. B.; Todd, A. R. *J. Chem. Soc.* **1964**, 1406–1412. (b) Mizuno, Y.; Endo, T.; Miyaoka, T.; Ikeda, K. *J. Org. Chem.* **1974**, *39*, 1250–1255.

Table II. NMR Properties of Caged Nucleotides

nucleotide	^{31}P NMR[a] chem shift, ppm α	β	γ	coupling const, Hz $J_{\alpha\beta}$	$J_{\beta\gamma}$	^{1}H NMR[b] chem shift, ppm: benzyl	coupling const, Hz: P-O-C-H or P-S-C-H
ATP	7.9 (d)	19.5 (t)	2.8 (d)	19	20		
caged ATP, I	8.3 (d)	20.3 (t)	9.4 (d)[c]	18	20	5.9	8.2
ATP(γ,S)	7.9 (d)	19.8 (dd)	-36.7 (d)	20	29		
S-caged ATP(γS), II	8.2 (d)	20.5 (dd)	-9.6 (sd)[c]	19	27	4.9	9.5
O-caged ATP(γ,S), III	8.3 (d)	21.0 (dd)	-45.2 (sd)[c]	19	27	6.0	8.2
ATP(β,γNH)	7.3 (d)	3.5 (dd)	-2.9 (d)	20	6		
caged ATP(β,γNH), IV	7.8 (dd)	8.2 (dd)	-1.6 (dd)[d]	19	6	N.D	7[d]

[a] Samples were prepared in 20% D_2O, 1 mM EDTA, pH 9.5, 21 °C. ATP(β,γNH) and IV were at pH 11. Spectra were recorded on a Bruker 200-MHz instrument at 81 MHz using a broad-band high-field probe and broad-band proton decoupler. Chemical shifts are relative to 85% H_3PO_4 using the sign convention of Jaffe and Cohn.[22a] Symbols in parentheses indicate the observed peak patterns: d = doublet, t = triplet, dd = doublet of doublets (due to spin coupling to two nuclei with different coupling constants), sd = split doublet (due to presence of diastereoisomers with different chemical shifts). [b] Spectra recorded in D_2O, pH 7, 25 °C on a Bruker 500-MHz instrument. The benzyl proton on the photolabile moiety of caged ATP could be assigned to a broad multiplet that collapsed to a triplet when the neighboring methyl protons were irradiated. This pattern is attributed to a pair of overlapping doublets due to coupling each diasteromeric proton to the γ-phosphorus. ^{31}P-^{1}H coupling constants were measured in these proton-decoupled spectra. Chemical shifts are relative to 3-(trimethylsilyl)propanesulfonate. [c] Alkylation gives rise to diastereoisomers that are expected to have slightly different chemical shifts. For caged ATP the chemical shift differences are too small for separate peaks to be observed. For S-caged ATP(γS) the chemical shifts are different by 14 Hz, giving rise to a split doublet. O-caged ATP(γS) represents four different compounds since a chiral center is formed at the γ-phosphate as well as at the benzyl carbon. Four doublets are possible, but only two are observed with a chemical shift difference of 8 Hz. [d] The P-O-C-H coupling constant for IV was estimated from ^{1}H-^{31}P-coupled ^{31}P spectra on a Bruker 400-MHz instrument. The γ-phosphorus resonance was a multiplet containing six peaks that is attributable to a diastereomeric pair of triplets. Triplets arise from coupling to the benzyl proton and the β-phosphorus with similar coupling constants (average splitting 7 Hz). Proton decoupling reduced the multiplicity to a split doublet (J = 7 Hz; chemical shift difference 14 Hz). The α-phosphorus resonance was a broad asymmetric multiplet that was poorly resolved in the coupled spectrum. Proton decoupling collapsed it to a split doublet (J = 19 Hz; chemical shift difference 9 Hz). The β-phosphorus resonance was unaffected by ^{1}H-^{31}P coupling and decoupling.

sulfonyl)hydrazones are converted to diazo compounds by alkaline decompostion.[20] As pointed out by Bamford and Stevens,[20a] alkaline treatment of tosylhydrazones of enolizable ketones can give rise to elimination. An attempted preparation of VII by this approach appeared to yield mostly 2-nitrostyrene.

In general, it is advantageous to prepare caged compounds with VII rather than (2-nitrophenyl)diazomethane since the photolytic byproduct 2-nitrosoacetophenone is less reactive and therefore less toxic to biological preparations than 2-nitrosobenzaldehyde. Furthermore, 1-(2-nitrophenyl)ethyl derivatives photolyze 20 times more rapidly in at least one case.[8]

Alkylation of a phosphate ester YPO_3H^- with VII leads to a caged compound VIII in high yield:

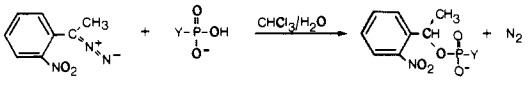

VII VIII

Caged ATP, prepared in approaching 100% yield, was shown to be identical with that prepared by the method of Kaplan et al.[2a] as characterized by analytical reversed-phase and ion-exchange HPLC, UV spectra, photochemical properties (Table I), and ^{31}P and ^{1}H NMR spectra (Table II). Yields of caged ATP were optimal when the aqueous phase was adjusted to pH 4 at the start of the reaction. This pH dependence suggests that the protonated phosphate group is the reactive species and is supported by the observation that the strongly acidic phosphate groups do not react under these conditions. Functional groups on the adenine and ribose rings also do not react in the two-phase system, a result confirmed by the absence of reactivity of adenosine under identical conditions. The reaction is also specific for weakly ionizing phosphate groups in other commonly encountered nucleotides: GTP, ITP, UTP, and CTP.

Solvents such as dimethyl sulfoxide are suitable for alkylations of cyclic nucleotides containing only strongly ionizing phosphate groups[5] and have been used to alkylate 3′,5′-cyclic AMP and 3′,5′-cyclic GMP with 1-(2-nitrophenyl)diazoethane (Wootten, J. F., Trentham, D. R., unpublished work). However, wherever possible the two-phase approach is the method of choice because it leads to good selectivity and high yields when alkylating phosphate monoesters and because of its general ease and convenience.[18d]

Radiolabeled caged ATP has been prepared from [2-^{3}H]ATP by treatment with VII (Ferenczi, M. A., Trentham, D. R., unpublished work). Until now, preparing labeled caged compounds has been difficult since intermediates in multistep syntheses are often not available in radiolabeled form (see for instance ref 4). Starting with radiolabeled biological substrates that are commercially available, the preparation of new labeled caged compounds should be rapid and efficient. This is an important consideration in the application of caged compounds to biological research.

Characterization of New Caged Compounds. Caged ATP(γS). Alkylation of ATP(γS) with VII presented a special problem, since the terminal phosphate possesses two different atoms, oxygen and sulfur, that can potentially react and the P^{3} atom is at a prochiral center. Caged ATP(γS) was resolved into two components by DEAE-cellulose chromatography, each of which liberated ATP(γS) as the only nucleotide photoproduct.[21] The first compartment eluted was S-caged ATP(γS), II, and the second, O-caged ATP(γS), III, based on the following analysis by NMR spectroscopy (Table II). The two components displayed characteristic α- and β-phosphate resonances, but the γ-phosphate resonances were at -9.6 and -45.2 ppm compared to -36.7 ppm for ATP(γS). Alkylated derivatives of phosphorothioate and adenosine 5′-phosphorothioate show that alkylation on sulfur causes an upfield change in chemical shift and alkylation on oxygen causes a downfield change relative to the parent compound.[22] This led to the above assignment of the two components, and ^{1}H NMR analysis corroborated this assignment. The benzyl proton on the 1-(2-nitrophenyl)ethyl moiety was found to resonate 1 ppm more upfield in S-caged ATP(γS) than in O-caged ATP(γS) or caged ATP (Table II). This is consistent with the observation that benzyl

(20) (a) Bamford, W. R.; Stevens, T. S. *J. Chem. Soc.* **1952**, 4735-4740. (b) Farnum, D. G. *J. Org. Chem.* **1963**, *28*, 870-872.

(21) Complete conversion of both O- and S-caged ATP(γS) to ATP(γS) was achieved by steady-state photolysis in the presence of 1 mM dithioerythritol. Under these or pulse photolysis conditions the sulfur in ATP(γS) did not detectably (by HPLC analysis) react with the photoproduct 2-nitrosoacetophenone nor was otherwise modified. In the absence of dithioerythritol the ATP(γS) formed was slowly modified.

(22) (a) Jaffe, E. K.; Cohn, M. *Biochemistry* **1978**, *17*, 652-657. (b) Eckstein, F.; Simonson, L. P.; Bar, H.-P. *Biochemistry* **1974**, *13*, 3806-3810. (c) Cummins, J. H.; Potter, B. K. L. *J. Chem. Soc., Chem. Commun.* **1985**, 851-853.

protons are shifted upfield when the benzylic group is bonded to sulfur as opposed to oxygen.[23]

Caged ATP(β,γNH). Reaction of ATP(β,γNH) with VII resulted in caged ATP(β,γNH) whose structure was verified as IV because photolysis of caged ATP(β,γNH) liberated ATP(β,γNH) as the only nucleotide product and by its ^{31}P NMR spectrum. However, the NMR spectrum of caged ATP(β,γNH) was more difficult to interpret than those of I–III. Three distinct ^{31}P signals were observed for both ATP(β,γNH) and caged ATP(β,γNH) at pH 11 (Table II); these were assigned by considering coupling between phosphorus atoms (J_{P-O-P} = 20 Hz, J_{P-N-P} = 6 Hz; see also ref 24). A direct comparison of spectra indicated that the β-phosphorus chemical shift was more affected by addition of the 1-(2-nitrophenyl)ethyl moiety (4.7 ppm change) than the γ-phosphorus (1.4 ppm change). This contrasts with similar spectral analyses of caged ADP, caged ATP, and caged ATP(γS) where the terminal phosphates undergo the largest change in chemical shift compared to the parent compounds (Table II). On the basis of this simple ^{31}P NMR analysis, the location of the caged group in caged ATP(β,γNH) is uncertain. This ambiguity was resolved by examining the effect of pH on the ^{31}P NMR spectra of ATP(β,γNH) and caged ATP(β,γNH), and by ^{1}H–^{31}P coupling experiments.

The ^{31}P NMR versus pH titration of ATP(β,γNH) was anomalous in the range pH 4–11 (see also ref 24a). In fact, the effects of protonation on chemical shifts were similar to the effects of alkylation described above. As the pH was decreased from pH 11, the β chemical shift moved 4.2 ppm downfield and the γ chemical shift moved 1.4 ppm downfield, and this raised a question concerning the precise location of the titratable proton in ATP(β,γNH). A detailed ^{17}O, ^{15}N, and ^{31}P NMR investigation of ATP(β,γNH) has shown that ionization of this proton occurs exclusively on the γ phosphate.[24b] In contrast to ATP(β,γNH), the spectrum of caged ATP(β,γNH) was unchanged over the range pH 4–11. Therefore, alkylation has most likely occurred on the weakly ionizing oxygen of the γ-phosphate. This conclusion was supported by the observation that only the α- and γ-phosphate atoms exhibited ^{1}H–^{31}P coupling (Table II), in the former case due to the 5′-methylene protons and in the latter to the benzyl proton.

Further evidence that O-caged ATP(γS), S-caged ATP(γS), and caged ATP(β,γNH) contained adenosine and 1-(2-nitrophenyl)ethyl moieties in a 1:1 ratio was based on the identity of their near-UV spectra with that of caged ATP. For each compound $\epsilon = 1.96 \times 10^4$ M^{-1} cm^{-1} at λ_{max} = 260 nm.

Quantum Yield and Photolysis Mechanism of Caged ATP. The product quantum yield, Q_p, of caged ATP was measured by direct comparison with that of caged P_i[2a] and found to be 0.63 (Table I), with error limits (estimated at ±10%) being primarily due to uncertainty in the value of Q_p for caged P_i. Q_p for caged ATP was independent of pH between pH 6 and 10.

The amount of ATP formed on laser pulse photolysis of caged ATP depends not only on Q_p but also on such factors as the lifetime of the excited state and the laser pulse width since these relate to the number of times a particular molecule may be excited.[4,25] A parameter that is likely to be directly related to the amount of ATP formed is the rapid initial absorption increase in the near-UV associated with the presumed *aci*-nitro intermediate. It follows that the extinction coefficient, ϵ, of this intermediate is an important constant, since the amount of caged ATP photolysis can be inferred from ϵ and the amplitude of the absorption transient. ϵ was therefore measured at its λ_{max} of 406 nm and at 380 nm, a wavelength used to monitor further processes associated with the photolysis (see below). The transient signal was compared with the absorption change at 740 nm that is associated

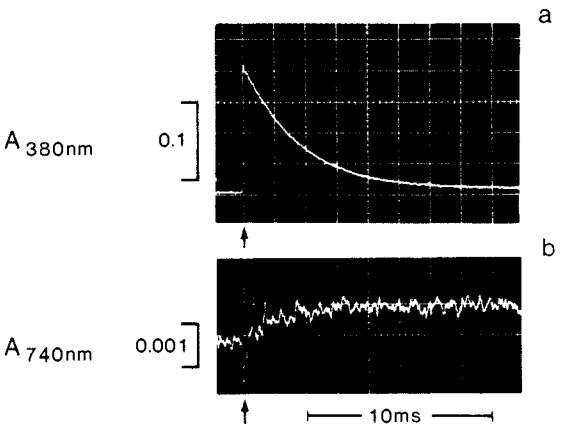

Figure 1. Kinetic records at (a) 380 nm and (b) 740 nm of laser pulse photolysis (irradiation at 320 nm) of caged ATP at 22 °C in an aqueous solution containing 1 mM caged ATP, 1 mM dithiothreitol, and 100 mM 2-(*N*-morpholino)ethanesulfonic acid (MES) adjusted to pH 6.7 with KOH. The arrows mark the time of the laser pulse. Longer time base records of the same reaction are shown in Figure 5a.

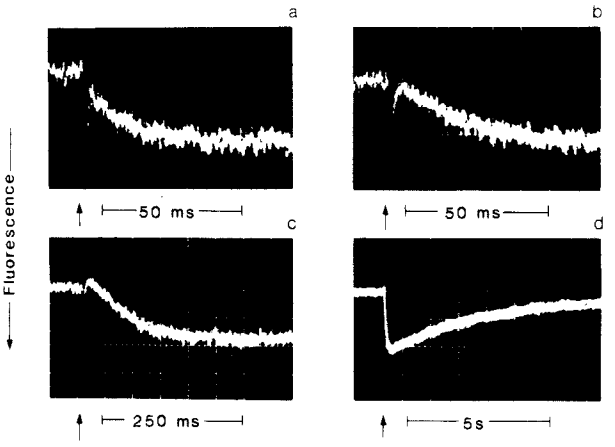

Figure 2. Records are of the reaction of 15 μM ATP released on photolysis of 1 mM caged ATP in the presence of 38 μM pyrene-labeled actin subfragment 1. Solution conditions: 0.4 mM $MgCl_2$, 0.5 mM dithiothreitol, ionic strength 0.08 M at 23 °C in buffers of MES, *N*-tris(hydroxymethyl)methyl-2-aminoethanesulfonic acid (TES), or tris(hydroxymethyl)aminomethane (Tris) at pH values 6.3, 7.0, and 7.9, for a–c, respectively. The 347-nm laser pulse was oriented 90° to the fluorescence excitation (366 nm) and emission (406 nm). 30% enhancement of pyrene fluorescence occurred in a–c. d is on a slow time scale to show that single turnover conditions pertain (i.e., as ATP is hydrolyzed, actin and subfragment 1 reassociate). Small arrows mark the time of the laser pulse.

with formation of XI for which ϵ_{740nm} = 50 M^{-1} cm^{-1}.[8] Figure 1 illustrates this. From this analysis $\epsilon_{380nm} = 6.3 \times 10^3$ cm^{-1} and $\epsilon_{406nm} = 9.1 \times 10^3$ M^{-1} cm^{-1}, with error limits (estimated as ±15%) being due primarily to uncertainty in ϵ_{740nm}.

Analysis of the mechanism of the photolysis of I is limited to a study of the dark reactions following the laser pulse. There are three products, ATP, 2-nitrosoacetophenone, and H^+, and so far there is one detectable intermediate. The kinetics associated with the formation and/or decay of each of these species was monitored.

The kinetics of formation of ATP was followed by use of a biological assay, taking advantage of the fact that ATP complexed with Mg^{2+} causes the dissociation of a pyrene-labeled actin–myosin (subfragment 1) complex.[26] The second-order rate constant of this ATP-induced dissociation was calculated from the rate of the pyrene fluorescence decay measured as a function of ATP concentration in a stopped-flow apparatus using the solvents and temperature described in Figure 2. The rate constant was 2×10^6 M^{-1} s^{-1} at each pH value. It the follows that if ATP is released in the presence of 38 μM pyrene-labeled actin subfragment 1 with

(23) Emsley, J. W.; Feeney, J.; Sutcliffe, L. H. *High Resolution Nuclear Magnetic Resonance Spectroscopy*; Pergamon: London, 1966; Vol. 2, p 1133.
(24) (a) Tran-Dinh, S.; Roux, M. *Eur. J. Biochem.* **1977**, *76*, 245–249. (b) Reynolds, M. A.; Gerlt, J. A.; Demou, P. G.; Oppenheimer, N. J.; Kenyon, G. L. *J. Am. Chem. Soc.* **1983**, *105*, 6475–6481.
(25) Greene, B. I.; Hochstrasser, R. M.; Weisman, R. B.; Eaton, W. A. *Proc. Natl. Acad. Sci. U.S.A.* **1978**, *75*, 5255–5259.
(26) Kouyama, T.; Mihashi, K. *Eur. J. Biochem.* **1981**, *114*, 33–38.

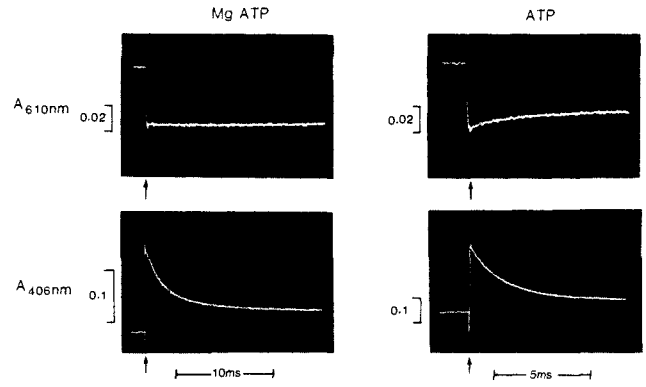

Figure 3. Kinetic records of laser pulse photolysis (irradiation at 320 nm) of caged ATP at 22 °C in the presence of the pH indicator bromothymol blue in an aqueous solution containing on the right 1 mM caged ATP, 50 μM bromothymol blue, 150 mM KCl, and 1 mM dithiothreitol and on the left solutions additionally containing 3 mM $MgCl_2$. The solutions were adjusted initially to pH 7, but the pH decreased following the laser pulse. Arrows mark the time of the laser pulse.

the proteins in significant molar excess, the fluorescence of the complex will decay exponentially with a rate constant of 76 s^{-1} if ATP release is very rapid (i.e. $\gg$76 s^{-1}) but at less than 76 s^{-1} if ATP release is partially or wholly rate limiting. The results show (Figure 2) that ATP release is significantly rate limiting at pH 7.9, partially rate limiting at pH 7.0, and not rate limiting at pH 6.3. The rate of the *aci*-nitro decay is first order in $[H^+]$ over this pH range.[26] Under the solvent conditions of the experiment described in Figure 2 the second-order rate constant was 1.25×10^9 M^{-1} s^{-1}, which leads to first-order rate constants for the *aci*-nitro decay of 16, 125, and 500 s^{-1} at pH values 7.9, 7.0, and 6.3, respectively. This strongly suggests that the rate of ATP formation is concomitant with the rate of the *aci*-nitro decay.

As already noted, there is an absorption change at 740 nm that has been ascribed to the formation of XI. The kinetics of appearance of the 740-nm band matched that of the *aci*-nitro decay as illustrated in Figure 1. This result rules out a mechanism previously suggested.[27] The extinction coefficients of nitroso groups are generally independent of the remainder of the molecule to which they are attached,[28] so that one cannot be sure whether the 740-nm signal is associated with XI formation or with a precursor containing a nitroso group such as XII. The following H^+-release results make it unlikely that XII is involved.

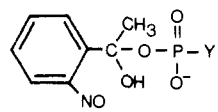

XII

H^+ release on laser pulse photolysis of I is rapid.[2b] This is shown in Figure 3. In this experiment changes in proton concentration were monitored at 610 nm through the H^+ indicator dye bromothymol blue (pK 7.0). In control experiments, the dye was not influenced by the laser pulse, so that none of the absorption change was due to dye bleaching. At pH 6.5, the triphosphate group of ATP contains no protons in the presence of Mg^{2+}; however, in the absence of Mg^{2+} it is partially protonated (for $ATP^{3-} \rightleftharpoons ATP^{4-} + H^+$, p$K_a$ = 6.5). In the absence of Mg^{2+} there was some H^+ uptake (illustrated in Figure 3) following the initial H^+ release.

Scheme I

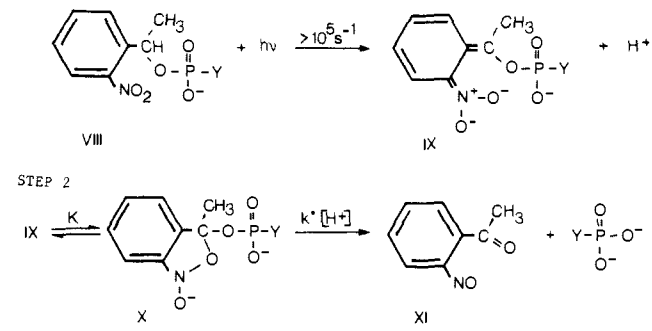

The rate of this uptake matched that of the *aci*-nitro decay, providing further evidence that the latter process occurs concomitant with ATP release. The results also rule out the possibility that the hemiketal XII builds up to a detectable level.[30] Hemiketal formation would give rise to H^+ uptake followed by H^+ release as it broke down to ATP and XI.

A minimal mechanism consistent with these kinetic results is shown in Scheme I. We propose that Scheme I may be applied to 1-(2-nitrophenyl)ethyl esters of phosphates containing a weakly acidic group such as P_i, AMP, ADP, ATP, and the ATP analogues derivatized here. We do not know as to how Scheme I, if valid, relates to the photolysis of 2-nitrobenzyl alcohols, aldehydes, and carboxylic acid esters. Scheme I incorporates intramolecular oxygen transfer that is known to occur on photolysis of *N*-acyl-8-nitrotetrahydroquinoline.[31] It is suggested that the *aci*-nitro compound is formed with a pK_a that is approximately 3.7 on the basis of studies with 2-nitrotoluene and other photochromic compounds.[32] However, our primary concern is to point out that at times >10 μs after the laser pulse only a single intermediate is kinetically resolvable. This intermediate may comprise a number of rapidly interconvertible forms such as IX and X.

The elimination of YPO_3^{2-} is proposed to occur in step 2 via a tetrahedral carbon intermediate, X (for the reason given in the introduction), that is in rapid equilibrium with IX. Rationalization of the acid catalysis of step 2 requires general-acid catalysis or protonation of IX or X. The most likely site for protonation is one of the nonbridging oxygen atoms in the $-YPO_3^-$ group of X, in which case the rate constant of the *aci*-nitro decay $k = Kk^*[H^+]/(1 + K)$, where k^* and K are defined in Scheme I.

Two further aspects of caged ATP photolysis bearing on the photolysis mechanism were studied and relate particularly to step 2 in Scheme I. The pH dependence of the *aci*-nitro decay rate was measured at higher pH values where one might expect the decay rate to become pH independent. The influence of Mg^{2+} on the *aci*-nitro decay was also studied further to see whether Mg^{2+} might cause the *aci*-nitro decay rate to be independent of pH by virtue of Mg^{2+} competition with H^+ for the nonbridging oxygen atoms in the $-YPO_3^-$ group of X. It is also important to know about the influence of Mg^{2+} for biological studies with these compounds since the intracellular free Mg^{2+} concentration is typically 1 mM.

The kinetics of the *aci*-nitro decay of caged ATP in the range pH 6.85–10 and in the presence of various concentrations of Mg^{2+} are shown in Figure 4. The reaction rates were proportional to $[H^+]$ below pH 9 but were independent of $[H^+]$ at pH 10. In the presence or absence of Mg^{2+} the rate constant of the *aci*-nitro decay at pH 10 was 1.5 s^{-1}, so that the pK_a of the leaving group (4.0 for $MgATP^{2-}$ and 6.5 for ATP^{4-})[33] had no effect on the rate

(27) We originally interpreted the photolysis mechanism of caged ATP in the presence of thiols on the basis of results obtained without using the 740-nm signal.[29] In those experiments, it was proposed that a process independent of thiol concentration (the 380-nm signal in Figure 5) represented the rate-limiting step in 2-nitrosoacetophenone formation. It was hypothesized that this process was the breakdown of an oxonium ion intermediate. This mechanism must be incorrect in view of the results shown in Figure 1.

(28) (a) Shors, A.; Kraaijeveld, E.; Havinga, A. *Recl. Trav. Chim. Pays-Bas* **1955**, *74*, 1243–1261. (b) Gowenlak, B. G.; Luttke, W. *Q. Rev. (London)* **1958**, *12*, 321–340.

(29) McCray, J. A.; Trentham, D. R. *Biophys. J.* **1987**, *51*, 447a.

(30) Chow, Y. L. In The Chemistry of Functional Groups. *The Chemistry of Amino Nitroso and Nitro Compounds and Their Derivatives*; Patai, S., Ed.; Wiley-Interscience: New York, 1982; Supplement F, Part 1, Chapter 6, pp 181–290.

(31) Amit, B.; Ben-Efraim, D. A.; Patchornik, A. *J. Chem. Soc., Perkin Trans. 1* **1976**, 57–63.

(32) (a) Wettermark, G.; Black, E.; Dogliotti, L. *Photochem. Photobiol.* **1965**, *4*, 229–239. (b) Margerum, J. D.; Miller, L. J. In *Photochromism, Techniques of Chemistry*; Brown, G. H., Ed.; Wiley-Interscience: New York, 1971; Vol. III, pp 557–632.

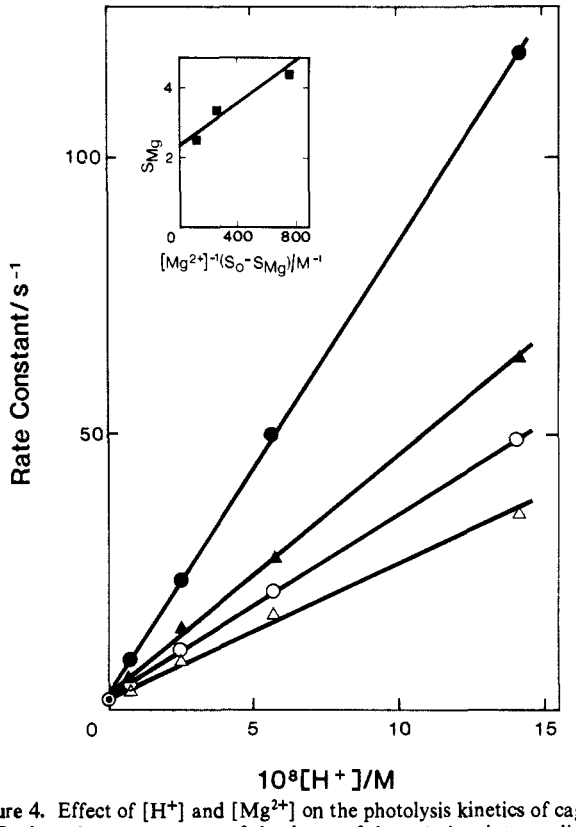

Figure 4. Effect of $[H^+]$ and $[Mg^{2+}]$ on the photolysis kinetics of caged ATP. k_{obs}, the rate constant of the decay of the *aci*-nitro intermediate, IX, was measured at 406 nm on photolysis of solutions containing 0.4 mM caged ATP at 22 °C. Mg^{2+} concentrations were as follows: ●, 0; ▲, 5 mM; ○, 20 mM; △, 50 mM. The buffer at pH 6.85, 7.24, 7.52, and 8.0 was 0.10 M TES adjusted to the required pH with KOH and at pH 10 was 0.10 M triethylamine adjusted with HCl. The solutions were made up to ionic strength 0.20 M with KCl. At pH 10, k_{obs} was measured in the presence of 0 and 20 mM Mg^{2+}. A secondary plot of the data is shown in the insert, where S_0 and S_{Mg} are slopes of the lines in the main part of the figure (see text). Linear least-square fits to the data were used to draw the lines.

of the non-acid-catalyzed reaction. The possibility that this pH-independent process is due to reversal of step 1 in Scheme I is ruled out by the fact that Q_p for caged ATP is the same at pH 6 and 10.

To analyze the data further, the equilibrium mixture of IX and X is termed AMg^{2-} or A^{4-}, depending on whether or not it is associated with Mg^{2+}. The kinetics of the decay of the *aci*-nitro intermediate may then be expressed as

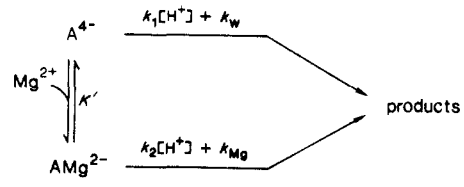

where k_1 and k_2 are second-order rate constants of the acid-catalyzed reactions and k_w and k_{Mg} are first-order rate constants of the uncatalyzed reactions. K' is the dissociation constant AMg^{2-}. Assuming that equilibrium between A^{4-} and AMg^{2-} is rapid, it follows that

$$k_{obs} = (1 + K'/[Mg^{2+}])^{-1}[k_2[H^+] + k_{Mg} + K'(k_1[H^+] + k_w)/[Mg^{2+}]] \quad (1)$$

where k_{obs} is the observed rate constant of the exponential *aci*-nitro decay. From the data at pH 10, $k_{Mg} = k_w = 1.5\ s^{-1}$, and from

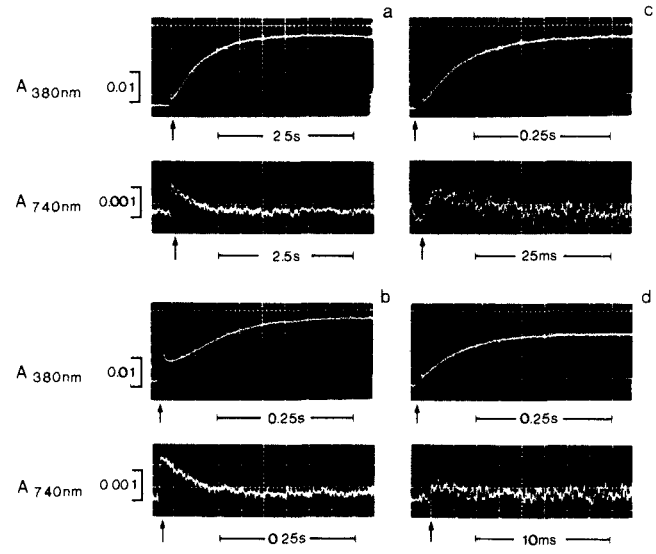

Figure 5. Influence of dithiothreitol on the laser pulse photolysis (irradiation at 320 nm) of caged ATP at 22 °C in the same solvent as in Figure 1 with thiol concentrations of (a) 1 mM, (b) 10 mM, (c) 0.10 M, and (d) 1.0 M. In each case upper records were obtained at 380 nm and lower records at 740 nm. In all cases the *aci*-nitro intermediate was observed as an initial absorption increase at 380 nm that decreased to almost zero by 20 ms as in Figure 1. Arrows mark the time of the laser pulse.

the data in the absence of Mg^{2+}, $k_1 = 8.3 \times 10^8\ M^{-1}\ s^{-1}$ (Figure 4). In addition, eq 1 can be rearranged and expressed as

$$k_2 = 10^8[S_{Mg} - K'(S_0 - S_{Mg})/[Mg^{2+}]]\ M^{-1}\ s^{-1}$$

where S_0 and S_{Mg} are the slopes of the lines in Figure 4 at zero and various Mg^{2+} concentrations. It then follows from graphical analysis that the ordinate intercept of the line in the inset of Figure 4 gives $k_2 = 2.35 \times 10^8\ M^{-1}\ s^{-1}$ and the slope of the line gives $K' = 3.0$ mM. The data are insufficient to be a stringent test of the above reaction scheme in the presence of Mg^{2+}, but they do strongly suggest that AMg^{2-} breaks down in an acid-catalyzed fashion below pH 10, though k_2 is 3.5-fold less than k_1. The proposed protonation of a nonbridging oxygen atom in X as a key feature of acid catalysis is not ruled out by this result since Mg^{2+} could presumably still form a complex with other anionic groups in X.

Reaction of 2-Nitrosoacetophenone with Thiols. The removal of the byproduct XI by thiols is an important aspect of the use of the laser pulse photolysis approach in biological systems. There is also the practical consideration that XI is insoluble in water and causes turbidity in aqueous solutions interfering with spectroscopic analysis. Reaction of XI with hydrophilic thiols avoids this problem. When the reaction shown in Figure 1 was monitored for longer times, further absorption changes occurred at 380 and 740 nm as shown in Figure 5a. A stopped-flow kinetic analysis of the reaction between dithiothreitol and XI or nitrosobenzene showed that the 740-nm signal was due to reaction of thiol with the nitroso group while the signal at 380 nm probably involves the ketone group as well. The remaining records of Figure 5 show how the rates of the 380- and 740-nm signals varied with dithiothreitol concentration.

The rate of decay of the 740-nm signal was first order in thiol concentration, and at 1 M dithiothreitol the nitroso group was removed as rapidly as it was formed (Figure 5d). On the other hand, the rate of the signal at 380 nm became independent of thiol as its concentration was increased. We conclude that initially the thiol reacted with the nitroso group, followed by a further reaction probably involving the ketone group. The processes shown in Figure 5 directly correlated with the reaction of dithiothreitol with XI as studied by stopped-flow. Thus, when XI was mixed with thiol at concentrations and with other solvent conditions as in Figure 5, identical records were observed at 380 nm after the first 50 ms to those seen in Figure 5. In addition, the stopped-flow

(33) Martell, A. E.; Schwarzenbach, G. *Helv. Chim. Acta* **1959**, *39*, 653–661.

analysis showed that the reaction between XI and thiol when monitored at 380 nm was a two-step process in which the initial reaction exhibited a small decrease in absorption (masked in the pulse photolysis studies by the signal from the *aci*-nitro decay as in Figure 1a). The difference spectrum in ethanol between the final reaction product mixture and XI showed a peak at 373 nm.

The kinetics of the two-step reaction of XI with dithiothreitol were studied at 380 nm over the range pH 6–8 by laser pulse photolysis of caged P_i. This is possible with caged P_i because the rate of release of XI is >8000 s^{-1} in this pH range (Table I). The second-order rate constant (derived from data at low (<10 mM) thiol concentration) was 3.5×10^3 M^{-1} s^{-1}, and the first-order rate constant was 45 s^{-1} at pH 7.0, 21 °C, and 0.18 M ionic strength. The rates of both steps were proportional to $[OH^-]$. The relatively high signal to noise ratio of the 740-nm signal in Figure 5a,b helps validate the signal in Figure 1b. The signal at 380 nm due to the reaction of XI and dithiothreitol is more than 1 order of magnitude greater than that at 740 nm and provides an easily monitored lower limit to the rate of XI formation on laser pulse photolysis of caged compounds.

Whether the process recorded at 380 nm that was independent of thiol concentration (as in Figure 5d) was specific to dithiothreitol was tested. Laser pulse photolysis of caged ATP was performed in the presence of reduced dithiotic acid[34] or 2-mercaptoethanol. In both cases the 380-nm signal was observed. In neither case was the rate of the process independent of concentration even at 1 M thiol, though in both cases the rates were less than first order in thiol at concentrations above 10 mM.

In practical terms for biological experiments the presence of thiol is important to act as a scavenger to compete with biomolecules for the nitrosoketone byproduct. Typically, 1–10 mM thiol is required for this purpose.[2a,35]

Photochemical Properties of New Compounds. On laser pulse photolysis, spectral intermediates were observed for compounds II–IV, which were analogous to the presumed *aci*-nitro intermediate described above for caged ATP. These intermediates were detected at 406 nm and decayed by a single-exponential process with rate constants (k in Table I) that depended linearly on $[H^+]$ near neutral pH (as shown in Figure 4 for caged ATP). As with caged ATP, Mg^{2+} decreased the k values for the caged ATP analogues but had little or no effect on the photolysis kinetics of caged AMP or caged P_i. II–IV also displayed uncatalyzed *aci*-nitro decay (measured at pH 10) with rate constants that were the same within experimental accuracy for caged ATP (1.5 s^{-1}). On the basis of the above spectroscopic kinetic analysis with caged ATP, first-order rate constants derived from the *aci*-nitro decay reaction were taken as a measure of photolysis rates for the new compounds (Table I).

The acid catalysis of *aci*-nitro decay is likely to be due to protonation of one of the nonbridging phosphate oxygens in X as discussed above for caged ATP. At pH 7.1, k values are different for compounds I–V (Table I) and, as indicated below, greater k values appear to correlate with weaker acidity of the ionized phosphate oxygen of X. Thus, in terms of Scheme I, any contribution the weaker acidity of the leaving group might have on reducing k^* is more than offset by the greater ease of protonation of X. Caged P_i, which has a pK_a of 6.8 (we assume this pK_a applies to protonation of X in Scheme I), has a k value that is 930-fold (~500-fold in the absence of Mg^{2+}) greater than for caged ATP whose pK_a is estimated as ~2 (from the pK_a of the strongly acidic groups of P_i and PP_i[36]).

Relative pK_a values of intermediates X of compounds I–IV were estimated by assuming that these values increase in the same order as the weakly acidic group of the uncaged nucleotide. The pK_a of ATP(γS)[11c,22a,37] is about 1 unit lower than that of ATP (pK_a = 6.5[33]), which is about 1 unit lower than ATP(β,γNH).[12a,24b] k values for the caged forms of these nucleotides for the most part increase with pK_a: S-caged ATP(γS), 35 s^{-1}; caged ATP, 86 s^{-1}; caged ATP(β,γNH), 250 s^{-1} (Table I). As indicated above, the fact that Mg^{2+} reduces k values for caged ATP and caged ATP analogues may reflect more difficult protonation of the critical oxygen atom in X. It should be noted however that O-caged ATP(γS) does not fit into this correlation between k values and pK_a.

Steady-state quantum yields, Q_p, were measured for compounds II–IV (Table I). Q_P is related to the extent of photolysis on laser pulse photolysis that is likely in turn to be directly proportional to the amplitude of the initial absorption change in the near-UV (as in Figure 1a). This is supported by the observation that relative values of Q_P and the absorption change (rel A_{406nm}) are equal within experimental limits of accuracy for each compound listed in Table I. The correlation indicates that the apparent $\epsilon_{406nm} = 9.1 \times 10^3$ M^{-1} cm^{-1} determined for the *aci*-nitro intermediate of caged ATP (Figure 1) is applicable to compounds II–V. However, this correlation may not generally be true because the chromophoric *aci*-nitro compound may be in equilibrium with other species and the equilibrium constants (e.g., K describing equilibration between IX and X in Scheme I) could vary from one compound to another.

Summary

A general method has been developed to introduce photolabile 1-(2-nitrophenyl)ethyl groups selectively into multifunctional molecules at weakly ionizing phosphate groups by use of 1-(2-nitrophenyl)diazoethane. Photolabile esters of commonly encountered nucleotides and the ATP analogues 5′-adenylyl imidodiphosphate (ATP(β,γNH)) and adenosine 5′-(3-thiotriphosphate) (ATP(γS)) were synthesized. Generalizing from results with the photolabile ester of ATP, photolysis occurs in two kinetically resolvable steps in aqueous solvents at neutral pH: first, the proton is released, and then the nucleotide and 2-nitrosoacetophenone.

The nucleotides were released photochemically from their respective precursors relatively rapidly and with high quantum yield. The release step is acid catalyzed, and the rate is reduced by up to a factor of 3.5 by Mg^{2+}. The new compounds represent useful new tools for initiating reactions with a millisecond time resolution in cellular and other organized biological preparations.

Acknowledgment. Supported by NIH Grant 18535 to the Pennsylvania Muscle Institute and by the Medical Research Council, U.K. J.A.M. was a Fogarty Senior International Fellow (1 F06 TW 00926-01) at the National Institute for Medical Research, 1984–1985. We thank Dr. H. Furumoto (Candela Laser Corp.) and Dr. M. A. Ferenczi for help in setting up the frequency-doubled dye laser.

(34) Wagner, A. F.; Walton, E.; Boxer, G. E.; Pruss, M. P.; Holly, F. W.; Folkes, K. *J. Am. Chem. Soc.* **1956**, *78*, 5079–5081.

(35) Goldman, Y. E.; Hibberd, M. G.; Trentham, D. R. *J. Physiol.* **1984**, *354*, 577–604.

(36) *Spec. Publ.–Chem. Soc.* **1964**, *No. 17*, 180, 190.

(37) Gerlt, J. A.; Reynolds, M. A.; Demou, P. C.; Kenyon, G. L. *J. Am. Chem. Soc.* **1983**, *105*, 6469–6474.